

Oxidation of *c*-axis-oriented epitaxial $\text{YBa}_2\text{Cu}_3\text{O}_{7-\delta}$ thin films in ozone-containing atmospheres

B.J. Gibbons^{a)}

*Superconductivity Technology Center, Los Alamos National Laboratory,
Los Alamos, New Mexico 87545*

C.B. Eom and R.A. Rao^{b)}

University of Wisconsin—Madison, Madison, Wisconsin 53706

S. Trolier-McKinstry and D.G. Schlom

The Pennsylvania State University, University Park, Pennsylvania 16802

(Received 26 July 2001; accepted 30 January 2002)

Oxygen diffusion into *c*-axis-oriented $\text{YBa}_2\text{Cu}_3\text{O}_{7-\delta}$ epitaxial thin films was observed using real-time spectroscopic ellipsometry. The experiments were conducted under controlled atmospheres of 10% O_3 /90% O_2 and 80% O_3 /20% O_2 . At 2×10^{-5} torr, oxidation of the films began at temperatures as low as 100–125 °C for heating rates ≤ 3 °C/min. Full oxidation was seen by 190 °C at these rates. Based on these data, the activation energy of oxygen diffusion into $\text{YBa}_2\text{Cu}_3\text{O}_{7-\delta}$ from an ozone/oxygen atmosphere was found to be between 0.43 and 0.52 eV. This was appreciably smaller than for in-diffusion in a molecular oxygen atmosphere. Higher ozone content atmospheres did not improve the oxidation kinetics. These atmospheres did, however, delay the onset of reduction in the films by 60–70 °C at higher temperatures.

I. INTRODUCTION

Josephson-effect devices using high-transition-temperature (T_c) superconductors, such as $\text{YBa}_2\text{Cu}_3\text{O}_7$, have demonstrated tremendous potential in applications such as superconducting quantum interference devices (SQUIDS) and ultrafast digital electronics. For example, a promising architecture for ultrafast analog-to-digital converters and other digital electronics is rapid single-flux quantum (RSFQ) logic.¹ Also, low- T_c -based SQUIDS are currently the most sensitive detectors of magnetic flux available.² The development of a reliable high- T_c Josephson junction technology would make such devices possible at liquid nitrogen temperatures. Despite this promise, and the continuing efforts to develop high- T_c technology, there are significant materials and processing challenges remaining to be overcome.

One of these challenges is to obtain smooth $\text{YBa}_2\text{Cu}_3\text{O}_{7-\delta}$ films with complete oxygenation all the way to the surface. Any oxygen deficiency on the scale of the coherence length results in a “dead” layer of non-superconducting material or material with depressed superconducting properties. This can significantly affect

the properties of a junction-based device. Thus, it is important to understand the process of oxidation so that high-quality $\text{YBa}_2\text{Cu}_3\text{O}_{7-\delta}$ films can be fabricated. There have been several studies on diffusion in bulk polycrystalline and single-crystal samples,^{3–23} as well as in oriented and epitaxial thin films.^{21,24–34} *In situ* resistivity (conductivity) measurements, thermogravimetry, secondary ion mass spectroscopy (SIMS) profiles of tracer diffusion, electrochemical measurements, internal friction measurements, and single wavelength ellipsometry have all been used to monitor the oxidation of the material. It should be noted that these studies were performed on samples of widely varying microstructural features, including porosity, grain size, twin density, orientation, sample surface area, impurity content, initial oxygen stoichiometry, and homogeneity of oxygen distribution. Thus, the values reported in the literature for the diffusion coefficient (D) and the activation energy (E_a) can, and do, vary significantly ($0.3 \text{ eV} \leq E_a \leq 2.3 \text{ eV}$).

In this work, we used real-time spectroscopic ellipsometry (RTSE) to study the oxygen in-diffusion behavior into sputtered *c*-axis-oriented $\text{YBa}_2\text{Cu}_3\text{O}_{7-\delta}$ epitaxial films on (001) SrTiO_3 substrates. It is well known that the optical properties of $\text{YBa}_2\text{Cu}_3\text{O}_{7-\delta}$ are strongly dependent upon the oxygen content.³⁵ In addition, it has been shown that spectroscopic ellipsometry

^{a)}e-mail: gibbons@lanl.gov

^{b)}Current address: Motorola, Austin, Texas

can be extremely sensitive to the oxygen content in $\text{YBa}_2\text{Cu}_3\text{O}_{7-\delta}$.³⁶ Therefore, RTSE was used to explore the kinetics underlying the oxygen diffusion behavior in these films.

II. EXPERIMENTAL PROCEDURE

The $\text{YBa}_2\text{Cu}_3\text{O}_{7-\delta}$ thin film samples studied in this work were deposited via 90° off-axis radio-frequency (rf)-magnetron sputtering.^{37,38} The substrates were (001)-oriented SrTiO_3 , and the films were 650 Å thick. This thickness was chosen such that the probing light would penetrate through the entire thickness of the film. During deposition, the substrate temperature was 720 °C and the total pressure was 200 mtorr ($\text{Ar}/\text{O}_2 = 4/1$). A root-mean-square (rms) roughness of 20 Å was determined via atomic force microscopy (AFM) measurements. The average grain size was ≈ 0.4 to $0.5 \mu\text{m}$ with a very uniform distribution. This was typical of all the samples studied. In addition, there was no evidence of surface precipitates or outgrowths on any of the films. For the oxidation experiments, the output from a commercial ozone generator (Model G1-L, PCI/Wedeco, West Caldwell, NJ) was used yielding a 10% O_3 and 90% O_2 mixture.³⁹ When high ozone content atmospheres were desired, an ozone distillation apparatus was used.⁴⁰ In this case, the purity of the ozone at the substrate position was measured to be $\approx 80\%$.⁴¹

Figure 1(a) shows a $\theta/2\theta$ x-ray diffraction pattern of an as-deposited film. Figure 1(b) shows a ϕ -scan of the 102 reflection of the same film. These plots are indicative of all of the films used in this study; all were (001)-oriented, epitaxial, and with a very small amount of oriented Y_2O_3 second phase. Additional ϕ -scans indicated the absence of any *a*-axis-oriented material. The films were also studied with x-ray diffraction subsequent to the oxidation experiments. In all cases minor differences were seen after the ozone treatments. For this reason, different samples were used for each heating rate to ensure the results were not dominated by sample history effects.

The RTSE used was a rotating polarizer-sample-fixed analyzer ($P_{\text{rot}}SA$) configuration. A complete description of the system can be found elsewhere.⁴² The wavelength range used covers 280 to 780 nm, and a full spectrum of data can be collected in as little as 34 ms. However, typically 40 optical cycles of the rotating polarizer were averaged, resulting in a full spectrum collection and data analysis time of 4 s.

III. RESULTS AND DISCUSSION

Initially, a sputtered $\text{YBa}_2\text{Cu}_3\text{O}_{7-\delta}$ film was reduced by heating the film to 500 °C at 1×10^{-7} torr (holding for 15 min) and allowing it to cool to room temperature.

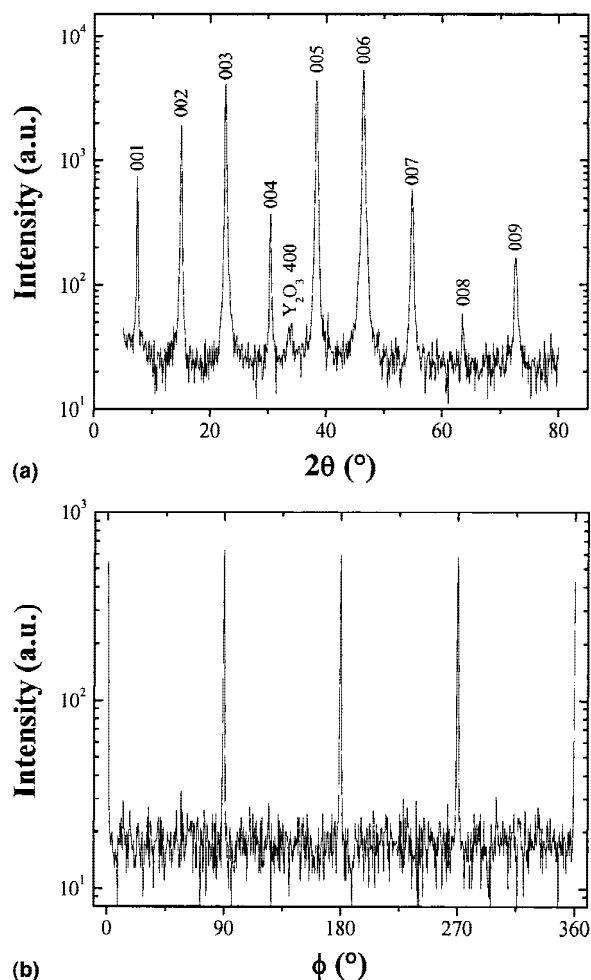


FIG. 1. (a) $\theta/2\theta$ x-ray diffraction pattern of an as-deposited $\text{YBa}_2\text{Cu}_3\text{O}_{7-\delta}$ film used in this study. (b) A ϕ -scan of the 102 reflection of the same film ($\phi \equiv 0^\circ$ along $\text{SrTiO}_3[001]$).

Next, the sample was heated at 1, 3, 5, 10, or 15 °C/min in 2×10^{-5} torr of the output from the ozone generator (10% $\text{O}_3/90\% \text{O}_2$). RTSE data were collected during these heating runs and are shown for selected heating rates in Figs. 2 and 3. In all cases, oxidation of the films was evident (for example by the overall rise in Ψ as a function of temperature for the range 500–780 nm). The onset of oxidation was apparent at lower temperatures for lower heating rates. Changes began to occur at temperatures as low as 100 °C for the slowest heating rate. At faster heating rates, less time was available at a given temperature for diffusion, so full oxidation of the films was pushed to higher temperatures.

The completion of oxidation was taken to correspond with the temperature at which the changes in the ellipsometric parameters slowed to the temperature dependence of Δ and Ψ . Figure 4 shows the 15 °C/min oxidation data at 550 nm compared to the temperature dependence of Ψ (at the same wavelength) for $\text{YBa}_2\text{Cu}_3\text{O}_6$ and $\text{YBa}_2\text{Cu}_3\text{O}_7$. It was clear that by 250 °C oxidation of the

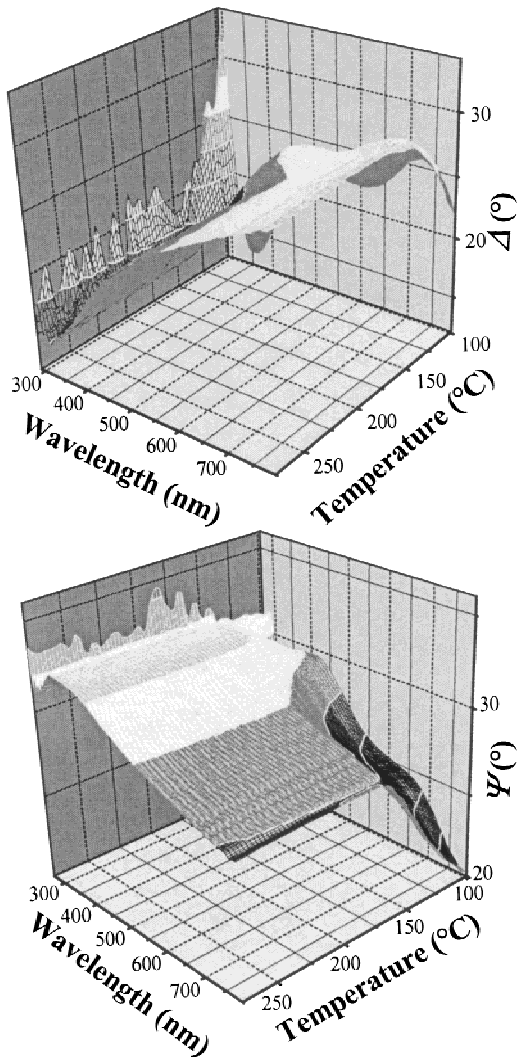


FIG. 2. Ellipsometric spectra of a reduced *c*-axis-oriented $\text{YBa}_2\text{Cu}_3\text{O}_{7-\delta}$ film heated at $1^\circ\text{C}/\text{min}$ in 2×10^{-5} torr of 10% $\text{O}_3/90\%$ O_2 .

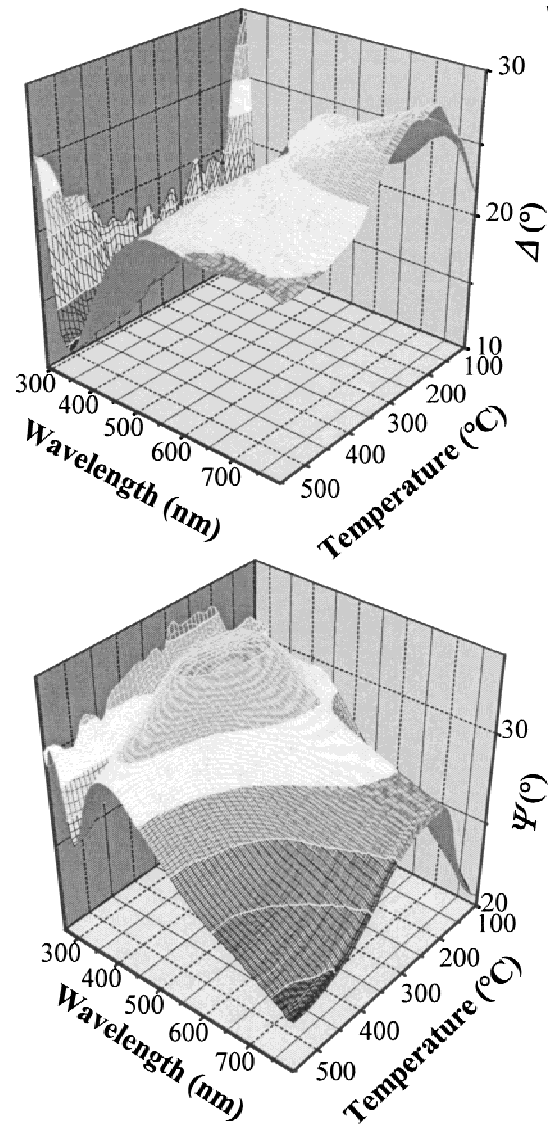


FIG. 3. Ellipsometric spectra of a reduced *c*-axis-oriented $\text{YBa}_2\text{Cu}_3\text{O}_{7-\delta}$ film heated at $5^\circ\text{C}/\text{min}$ in 2×10^{-5} torr of 10% $\text{O}_3/90\%$ O_2 .

film was completed, and the remaining temperature dependence (up to $\approx 310^\circ\text{C}$) was due to the temperature dependence of the $\text{YBa}_2\text{Cu}_3\text{O}_7$ dielectric properties. Consequently, the activation energy of oxygen diffusion into a sputtered $\text{YBa}_2\text{Cu}_3\text{O}_{7-\delta}$ film in a 10% $\text{O}_3/90\%$ O_2 atmosphere could be determined by measuring the temperature at which oxidation was complete as a function of the heating rate.

To do this, the analysis of Tu *et al.*¹¹ for diffusion in bulk $\text{YBa}_2\text{Cu}_3\text{O}_{7-\delta}$ was used. J is defined as the number of diffusing oxygen atoms per square centimeter, N_v is the number of oxygen atoms in the CuO layer per cubic centimeter, and δ is the fraction of missing oxygen atoms in the CuO layer (where $0 \leq \delta \leq 1$). If non-steady-state diffusion is assumed, the total number of oxygen atoms diffused into the oxide per unit area over a time period t_o is given by¹¹:

$$N_v \delta = \int_0^{t_o} -(\nabla \cdot J) dt \quad , \quad (1)$$

where

$$J = -D \frac{\partial(N_v \delta)}{\partial x} \quad , \quad (2)$$

and

$$D = D_o \exp[-E_a/kT] \quad . \quad (3)$$

Here D is the diffusivity in the film, and E_a is the activation energy for diffusion into the film. One can then change the base from time to temperature, and assuming one-dimensional diffusion obtain¹¹:

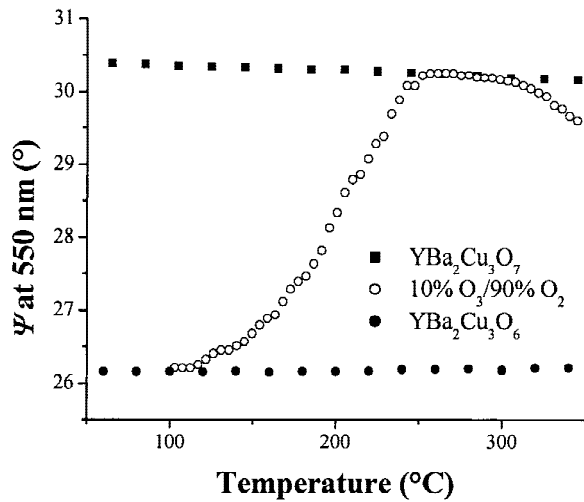


FIG. 4. Constant-wavelength trace at 550 nm of $\text{YBa}_2\text{Cu}_3\text{O}_6$, $\text{YBa}_2\text{Cu}_3\text{O}_7$, and an initially oxygen-deficient film heated in 10% $\text{O}_3/90\% \text{O}_2$ (all taken at $15^\circ\text{C}/\text{min}$). This plot indicates that the changes in the ellipsometric parameters beyond the point of complete oxidation are due to the temperature dependence alone.

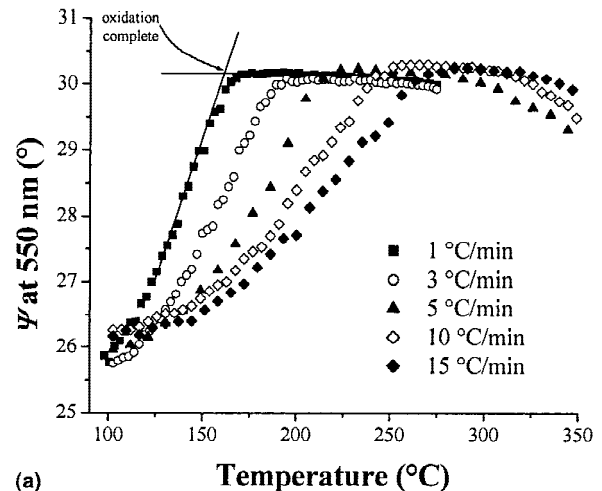
$$\delta = \int_{RT}^{T_{\max}} D \left(\frac{\partial^2 \delta}{\partial x^2} \right) \left(\frac{dT}{dT} \right) dT, \quad (4)$$

where RT is room temperature and T_{\max} is the temperature at which the changes in the ellipsometric spectra are no longer due to oxygenation of the film. At a constant heating rate, the solution of Eq. (4) can be found from the thermal analysis of Kissinger⁴³ and Ozawa⁴⁴ to be

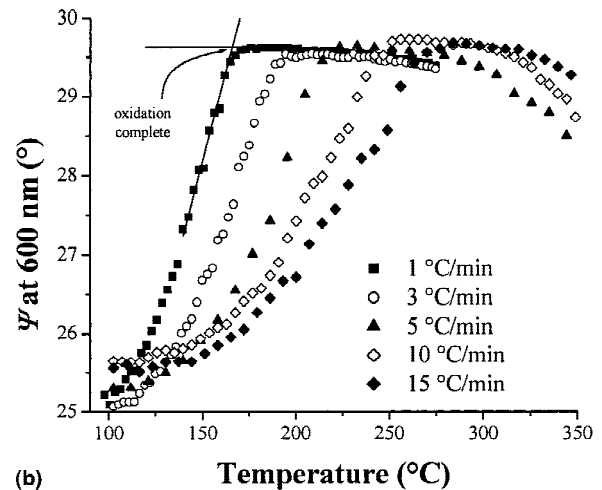
$$\delta \left(\frac{dT}{dt} \right) = \left(D_o \frac{\partial^2 \delta}{\partial x^2} \right) \left(\frac{kT_{\max}^2}{E_a} \right) \exp[-E_a/kT_{\max}]. \quad (5)$$

In solving for Eq. (5), E_a was assumed to be constant and $\partial^2 \delta / \partial x^2$ to be a slowly varying function of temperature.¹¹ The first assumption is justified on the basis that a near-surface layer saturated with oxygen forms in the early stage of oxidation, and this layer limits the in-diffusion of oxygen with a constant activation energy.¹¹ Although this layer thickens with time, the oxygen concentration gradient does not vary much, so the second assumption would also be satisfied.

From Eq. (5), E_a can be determined by plotting either $\ln[(dT/dt)/T_{\max}^2]$ versus $1/kT_{\max}$ or by plotting $\ln(dT/dt)$ versus $1/kT_{\max}$, since T_{\max} does not vary much as compared to the heating rate. First, T_{\max} was determined from constant-wavelength traces taken from each of the heating rates (see Fig. 5). To obtain T_{\max} , best fit lines were drawn to the data before and after the changes due to oxidation ceased. This was done for several different wavelengths at each heating rate; the obtained temperatures varied less than 10°C . Figure 6 shows the results of the two different approaches to calculating E_a . The lines



(a) Temperature ($^\circ\text{C}$)



(b) Temperature ($^\circ\text{C}$)

FIG. 5. Constant-wavelength traces of the ellipsometric parameter Ψ taken at (a) 550 nm and (b) 600 nm. These plots were used to determine when the changes in the ellipsometric parameters were no longer due to oxidation of the films.

are least-squares linear fits to the data. The good fit suggests that the assumptions made in the analysis are reasonable. The slopes give activation energies of 0.52 and 0.43 eV for oxygen diffusion in an O_3/O_2 atmosphere. For thin film *c*-axis-oriented $\text{YBa}_2\text{Cu}_3\text{O}_{7-\delta}$, Yamamoto *et al.*³¹ extracted activation energies of 1.2 eV from oxidation experiments in molecular oxygen and 0.65 eV from oxidation experiments in atomic oxygen generated by an electron cyclotron resonance plasma source. These energies were obtained through *in situ* resistivity measurements. Thus, the values obtained for an ozone atmosphere here agree well with the value observed for the mixture of atomic and molecular oxygen used by Yamamoto *et al.*³¹

For the slowest heating rates (1 and $3^\circ\text{C}/\text{min}$), complete oxidation is seen below 190°C . The typical practice to fully oxygenate $\text{YBa}_2\text{Cu}_3\text{O}_{7-\delta}$ films has been to hold at $400\text{--}450^\circ\text{C}$ for a period of time in a high-pressure O_2 environment subsequent to deposition.⁴⁵

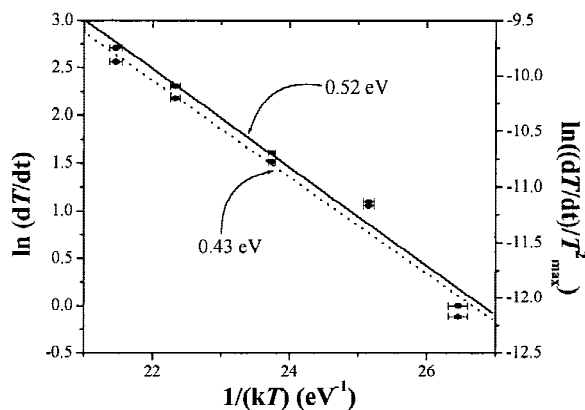


FIG. 6. Plots of $\ln(dT/dt)$ and $\ln[(dT/dt)/T_{\max}^2]$ versus $1/kT_{\max}$ for five different heating rates. The slopes of the curve-fitted lines give the activation energy for diffusion of oxygen into $\text{YBa}_2\text{Cu}_3\text{O}_{7-\delta}$ from a 10% $\text{O}_3/90\%$ O_2 atmosphere.

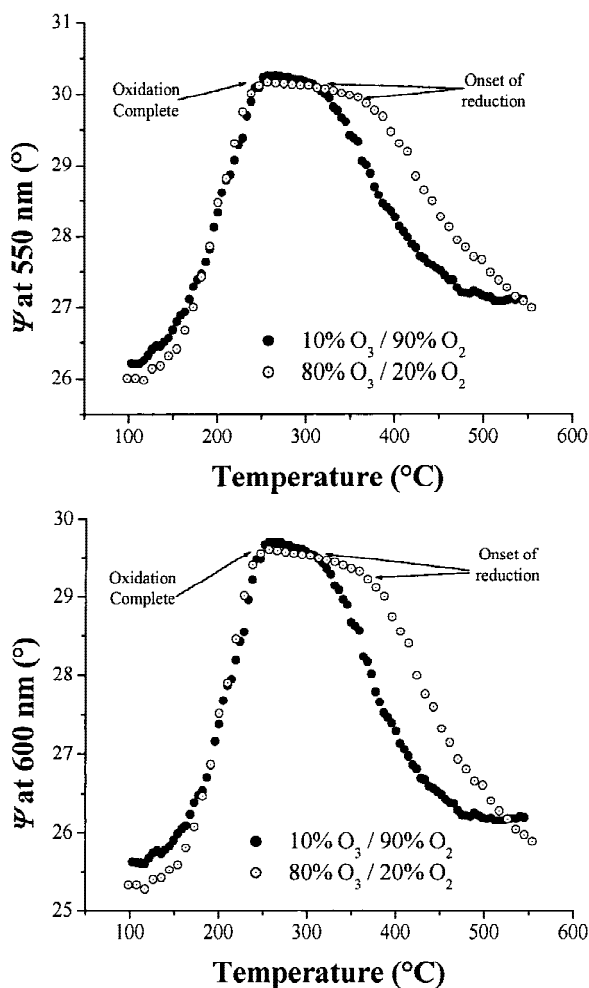


FIG. 7. Constant-wavelength traces in Ψ (at 550 and 600 nm) from a sputtered $\text{YBa}_2\text{Cu}_3\text{O}_{7-\delta}$ film heated at $10^\circ\text{C}/\text{min}$ in 10% $\text{O}_3/90\%$ O_2 (output from the ozone generator) and 80% $\text{O}_3/20\%$ O_2 (distilled output from the ozone generator).

These data indicate that the same films can be oxidized at much lower temperatures when using an ozone/oxygen atmosphere.

Finally, the effects of an 80% $\text{O}_3/20\%$ O_2 atmosphere were examined (the distilled output from the ozone generator). Initially, the film was heated at $10^\circ\text{C}/\text{min}$ in 2×10^{-5} torr and the data were compared to those for the same heating rate in the ozone generator output atmosphere (10% $\text{O}_3/90\%$ O_2). Constant-wavelength traces are shown in Fig. 7 for the two different atmospheres. It can be seen that there is essentially no difference in the value of T_{\max} for the two conditions. This indicates that at these low temperatures, the output from the ozone generator alone is sufficient to oxidize the film. However, at higher temperatures, the difference between the two atmospheres is marked. The purer ozone atmosphere delays reduction in the film until higher temperatures are reached. In general, the 80% ozone mixture delays the onset of reduction by $60\text{--}70^\circ\text{C}$. It is clear that simply supplying more ozone to the film surface does not lower the activation energy for oxygen in-diffusion. This is an indication that the measured activation energy results from oxygen transfer through a near-surface layer saturated with oxygen, as opposed to energy needed to break down the ozone at the surface of the film.

IV. CONCLUSION

The activation energy of oxygen diffusion into $\text{YBa}_2\text{Cu}_3\text{O}_{7-\delta}$ from an ozone/oxygen atmosphere was determined using RTSE. E_a was found to be between 0.43 and 0.52 eV. These values are about half of those reported for in-diffusion from a molecular oxygen atmosphere. Changes in the RTSE parameters due to oxidation were seen at temperatures as low as 100°C for the slowest heating rates. This is an indication that ozone can be used to fully oxidize $\text{YBa}_2\text{Cu}_3\text{O}_{7-\delta}$ films at temperatures much lower than currently used for molecular oxygen anneals.

ACKNOWLEDGMENT

The authors gratefully acknowledge funding from the Office of Naval Research (ONR) through Contract Nos. N00014-94-1-0815 and N00014-95-1-0513.

REFERENCES

1. K.K. Likharev, in *The New Superconducting Electronics*, edited by H. Weinstock and R.W. Ralston (Kluwer, Dordrecht, Germany, 1993).
2. J. Clarke, in *The New Superconducting Electronics*, edited by H. Weinstock and R.W. Ralston (Kluwer, Dordrecht, Germany, 1993).
3. K.N. Tu, S.I. Park, and C.C. Tsuei, *Appl. Phys. Lett.* **51**, 2158 (1987).
4. K.N. Tu, C.C. Tsuei, S.I. Park, and A. Levi, *Phys. Rev. B* **38**, 772 (1988).

5. B.A. Glowacki, R.J. Highmore, K.F. Peters, A.L. Greer, and J.E. Evetts, *Supercond. Sci. Technol.* **1**, 7 (1988).
6. K.N. Tu, N.C. Yeh, S.I. Park, and C.C. Tsuei, *Phys. Rev. B* **38**, 5118 (1988).
7. V.A.M. Brabers, W.J.M. de Jonge, L.A. Bosch, C. van der Steen, A.M.W. de Groot, A.A. Verheyen, and C.W.H.M. Vennix, *Mater. Res. Bull.* **23**, 197 (1988).
8. N.C. Yeh, K.N. Tu, S.I. Park, and C.C. Tsuei, *Phys. Rev. B* **38**, 7087 (1988).
9. D.J. Vischjager, P.J. Van der Put, J. Schram, and J. Schoonman, *Solid State Ionics* **27**, 199 (1988).
10. Y. Ikuma and S. Akiyoshi, *J. Appl. Phys.* **64**, 3915 (1988).
11. K.N. Tu, N.C. Yeh, S.I. Park, and C.C. Tsuei, *Phys. Rev. B* **39**, 304 (1989).
12. S.J. Rothman, J.L. Routbort, and J.E. Baker, *Phys. Rev. B* **40**, 8852 (1989).
13. H.L. Tuller and E. Opila, *Solid State Ionics* **40/41**, 790 (1990).
14. J. Maier, P. Murugaraj, and G. Pfundtner, *Solid State Ionics* **40/41**, 802 (1990).
15. J.L. Tallon and M.P. Staines, *J. Appl. Phys.* **68**, 3998 (1990).
16. Y. Scolnik, E. Sabatani, and D. Cahen, *Physica C* **174**, 273 (1991).
17. T.B. Tang and W. Lo, *Physica C* **174**, 463 (1991).
18. P. Schleger, W.N. Hardy, and B.X. Yang, *Physica C* **176**, 261 (1991).
19. S.I. Bredikhin, G.A. Emel'chenko, V.S. Shechtman, A.A. Zhokhov, S. Carter, R.J. Chater, J.A. Kilner, and B.C.H. Steele, *Physica C* **179**, 286 (1991).
20. J.L. MacManus, D.J. Fray, and J.E. Evetts, *Physica C* **190**, 511 (1992).
21. C. Krauns and H-U. Krebs, *Z. Phys. B* **92**, 43 (1993).
22. J.R. LaGraff and D.A. Payne, *Physica C* **212**, 470 (1993).
23. K. Conder and C. Krüger, *Physica C* **269**, 92 (1996).
24. W.A.M. Aarnink, R.P.J. IJsselsteijn, J. Gao, A. van Silfhout, and H. Rogalla, *Phys. Rev. B* **45**, 13002 (1992).
25. M.E. Bijlsma, Ph.D. Thesis, University of Twente, Enschede, The Netherlands (1996).
26. E.A.F. Span, H. Wormeester, D.H.A. Blank, and H. Rogalla, *Mater. Sci. Eng. B* **56**, 123 (1998).
27. A. Bock, R. Kürsten, M. Brühl, N. Dieckmann, and U. Merkt, *Phys. Rev. B* **54**, 4300 (1996).
28. G. Sageev-Grader, P.K. Gallagher, J. Thomson, and M. Gurvitch, *Appl. Phys. A* **45**, 179 (1988).
29. A. Yoshida, H. Tamura, S. Morohashi, and S. Hasuo, *Appl. Phys. Lett.* **53**, 811 (1988).
30. Q.Y. Ying, H.S. Kim, D.T. Shaw, and H.W. Kwok, *Appl. Phys. Lett.* **55**, 1041 (1989).
31. K. Yamamoto, B.M. Lairson, J.C. Bravman, and T.H. Geballe, *J. Appl. Phys.* **69**, 7189 (1991).
32. S.H. Lee, S.C. Bae, J.K. Ku, and H.J. Shin, *Phys. Rev. B* **46**, 9142 (1992).
33. Y. Li, J.A. Kilner, T.J. Tate, M.J. Lee, R.J. Chater, H. Fox, R.A. De Souza, and P.G. Quincey, *Phys. Rev. B* **51**, 8498 (1995).
34. Y.P. Li, J.R. Liu, W.K. Chu, J.A. Kilner, and T.J. Tate, in *Proc. 14th Int. Conf. on the Application of Accelerators in Research and Industry*, edited by J.L. Duggan and I.L. Morgan (AIP, Woodbury, NY, 1996), p. 693.
35. J. Kircher, M.K. Kelly, S. Rashkeev, M. Alouani, D. Fuchs, and M. Cardona, *Phys. Rev. B* **44**, 217 (1991).
36. B.J. Gibbons and S. Trolrier-McKinstry, *Thin Solid Films* **352**, 205 (1999).
37. C.B. Eom, J.Z. Sun, K. Yamamoto, A.F. Marshall, K.E. Luther, T.H. Geballe, and S.S. Laderman, *Appl. Phys. Lett.* **55**, 595 (1989).
38. C.B. Eom, J.Z. Sun, B.M. Lairson, S.K. Streiffer, A.F. Marshall, K. Yamamoto, S.M. Anlage, J.C. Bravman, and T.H. Geballe, *Physica C* **171**, 354 (1990).
39. C. Kraisinger, M.S. Thesis, The Pennsylvania State University, University Park, PA (1996).
40. D.G. Schlom and J.S. Harris, Jr., in *Molecular Beam Epitaxy: Applications to Key Materials*, edited by R.F.C. Farrow (Noyes Publications, Park Ridge, NJ, 1995), p. 505.
41. C.D. Theis and D.G. Schlom, in *High Temperature Materials Chemistry IX*, edited by K.E. Spear (Electrochemical Society, Pennington, 1997), Vol. 97-39, p. 610.
42. B.J. Gibbons, M.E. Hawley, S. Trolrier-McKinstry, and D.G. Schlom, *J. Vac. Sci. Technol. A* **19**, 584 (2001).
43. H.E. Kissinger, *Anal. Chem.* **29**, 1702 (1957).
44. T. Ozawa, *J. Therm. Anal.* **2**, 301 (1970).
45. See for example, *Science and Technology of Thin Film Superconductors II*, edited by R.D. McConnell and R. Noufi (Plenum, New York, 1990).